C. R. Palevol 9 (2010) 455–461

Contents lists available at ScienceDirect

Comptes Rendus Palevol

www.sciencedirect.com

General palaeontology

Finite element analysis: A promising tool for the reconstruction of extinct vertebrate graviportal taxa. A preliminary study based on the metacarpal arrangement of *Elephas maximus*

Analyse par éléments finis: un outil prometteur pour la reconstruction de taxons graviporteurs de vertébrés disparus. Étude préliminaire fondée sur l'arrangement métacarpien d'Elephas maximus

Florent Goussard[a,*], Damien Germain[a,b], Cyrille Delmer[c], Karen Moreno[d,e,f]

[a] *Muséum national d'histoire naturelle, département histoire de la terre, USM 0208-UMR 7207 CNRS CR2P « centre de recherche sur la paléobiodiversité et les paléoenvironnements », case postale 38, 57, rue Cuvier, 75231 Paris cedex 05, France*
[b] *Équipe de recherche, « évolution des vertébrés et paléoenvironnements », faculté des sciences Semlalia, Marrakech, Morocco*
[c] *Palaeontology Department, Natural History Museum, London, United Kingdom*
[d] *Computational Biomechanics Research Group, University of New South Wales, Sydney, Australia*
[e] *Instituto de Geociencias, Universidad Austral de Chile, Casilla 567, Valdivia, Chile*
[f] *Laboratoire d'anthropologie moléculaire et imagerie de synthèse (CNRS – FRE 2960), université Paul-Sabatier, 39, allée Jules-Guesde, 31073 Toulouse, France*

ARTICLE INFO

Article history:
Received 10 March 2010
Accepted after revision 30 July 2010
Available online 30 October 2010

Written on invitation of the Editorial Board

Keywords:
Biomechanics
Functional morphology
Metacarpal arrangement
Finite element analysis
Stress distribution

ABSTRACT

Finite element analysis (FEA) is a powerful tool to characterize the functional behaviour of bone. Here we use this technique to study the metacarpal arrangement of the Asian elephant. The objective of this work is to search for valid criteria that distinguish the known natural arrangement among a variety of configurations, including some fictitious ones. FEA yields significant statistical differences within the three arrangements tested. Our calculations suggest that the median value of stress (von Mises) could be a discriminant criterion, at least in graviportal taxa. Such a method could thus be applied to other graviportal organisms such as sauropod dinosaurs.

Mots clés :
Biomécanique
Morphologie fonctionnelle
Arrangement métacarpien
Analyse en éléments finis
Distribution du stress

RÉSUMÉ

L'analyse par éléments finis (FEA) est un outil puissant permettant de caractériser le comportement fonctionnel de l'os. Nous proposons ici d'utiliser cette technique pour étudier l'arrangement métacarpien de l'éléphant d'Asie, dans le but de mettre en évidence un critère valide permettant de caractériser l'arrangement naturel connu parmi plusieurs possibilités, dont certaines fictives. L'analyse en éléments finis réalisée ici révèle des différences statistiques significatives entre trois arrangements testés, et suggère que la valeur médiane de stress (von Mises) pourrait être

* Corresponding author.
E-mail addresses: goussard@mnhn.fr (F. Goussard), dinohuella@yahoo.com (K. Moreno).

1631-0683/$ – see front matter
doi:10.1016/j.crpv.2010.07.009

un critère discriminant, au moins chez les taxons graviporteurs. Une telle méthode pourrait donc être appliquée à d'autres organismes graviporteurs tels que les dinosaures sauropodes.

1. Introduction

Even if several complete skeletons of extinct taxa are known, the possible arrangements of the preserved bones, especially their limbs, can remain ambiguous in absence of discernible articular facet. Therefore, the reconstruction of their body and posture are highly debatable. For example, the lesser degree of ossification of articular facets in dinosaurs leads to a debate on their stance and gait (Paul and Christiansen, 2000). Indeed, slight differences in the relative positions of bones may have an additive effect over several joints and lead to distinct reconstructions of the same animal (Christian and Preuschoft, 1996). Even though the discovery of articulated skeletons helps to limit the range of possibilities, this type of preservation is not abundant enough to give hints on the much larger amount of non-articulated specimens.

In this context, it becomes fundamental to search for appropriate criteria that could allow testing and verification of the reconstructions of extinct animals. We believe this is possible because different bone arrangements necessarily lead to different stress patterns (Christian and Preuschoft, 1996). Therefore, the comparison between stress distributions in bones of an extant animal with a known arrangement at a variety of configurations, including some fictitious ones, may reveal the signature that characterizes the real bone arrangement. Then, applied on extinct taxa, the analysis of the stress distribution may be a valid criterion to test the plausibility of different hypothetical reconstructions.

Improvement of computing performance of finite element analysis (FEA) now makes it possible to use this as a virtual experimental platform to analyze diverse bone arrangements. By allowing the calculation of the stress distribution in virtually loaded bones, FEA makes it possible today to go farther in the understanding of the functional behaviour of skeletal elements (Rayfield, 2007; Richmond et al., 2005). For example, it has been extensively used to study the feeding mechanics in extant and/or extinct taxa (Dumont et al., 2005; Dumont, 2007; Kupczik et al., 2009; Moazen et al., 2008; Moreno et al., 2008; Tanner et al., 2008; Wroe, 2008; Wroe et al., 2008). Also, numerous studies on the appendicular skeleton using FEA have been used for the clinical assessment of humans, equids and bovines, as well as the estimation of the material properties of different tissues (Anderson et al., 2007; Carrigan et al., 2003; Dar and Aspden, 2003; Reggiani et al., 2006; Wu, 2007), while there are fewer on the study of the evolution of posture (e.g. Moreno et al., 2007; Richmond, 2007).

The purpose of the present study is to investigate parameters provided by FEA on how the metacarpal arrangement of an Asian elephant, *Elephas maximus*, can be deduced from the comparative stress distributions calculated from various FE models, including hypothetical ones, as if its real arrangement was unknown. Furthermore, we investigate the role of the metacarpal arrangement in the control of internal and external forces during the static weight-bearing phase. The model used in this study, *E. maximus*, is one of the largest modern graviportals. Therefore, its limb structure (including metacarpus) is primarily designed to meet the problem of bearing weight (Coombs, 1978). Other graviportals such as the extinct sauropod dinosaurs needed to cope with the same mechanical problem and so we believe that our method will provide a means for the deduction of their posture as well.

2. Material and methods

The metacarpus used in the present study is from a fresh limb of *E. maximus* (Asian elephant). No further information about this specimen is available, including the age, size or sex (Hutchinson, com. pers.), but for size we believe it is a sub adult. A 3D FE computer simulation of the metacarpus was generated on the basis of Computerized Tomography X-ray (CT) scan data. CT scanning was conducted at the Royal Veterinary College, University of London, using a Picker International Inc. PQ50,000 scanner (acquisition parameters: 120 kV, 200 mAs). Slices are 0.938 mm thick with an inter-slice distance of 1.74 mm, and a field of view (FoV) of 480 mm diameter (300 slices in total). Surface meshes are generated from CT data and then converted to solid meshes using Materialise MIMICS™ software (v13.1, 2009). Each metacarpal is meshed separately and converted into a 366,026 'brick' element model, with each element modelled as low order (four-noded) tetrahedral 'brick'. We focused on modelling the bone, rather than soft tissue, because the aim of the present work is to provide information for fossilized skeletons that will not have soft tissues preserved. Indeed, soft tissue is an important factor controlling the distribution of forces, and its inclusion in the model is likely to drastically modify bone loading. However, we base our study on the reasonable assumption that bones are morphologically adapted to their posture; therefore, they will be generally under lower stress if placed at the correct orientation (Fig. 1).

We performed FEA in order to examine stress distributions within the elephant metacarpus with the software STRAUS7 v2.3, 2004™, under the following conditions:

- the models are aligned with the general coordinate system. Each metacarpal remains as single objects, which are only connected at the proximal end by multiple rigid links. These rigid links coerce even distribution of force within the connected nodes, therefore simulating the wrist joint as a solid, static carpal assemblage (Fig. 1A, B). In order to evaluate the changes of stress distribution due to the metacarpal arrangement, three different models are generated, using STRAUS7 software (v2.3, 2004):

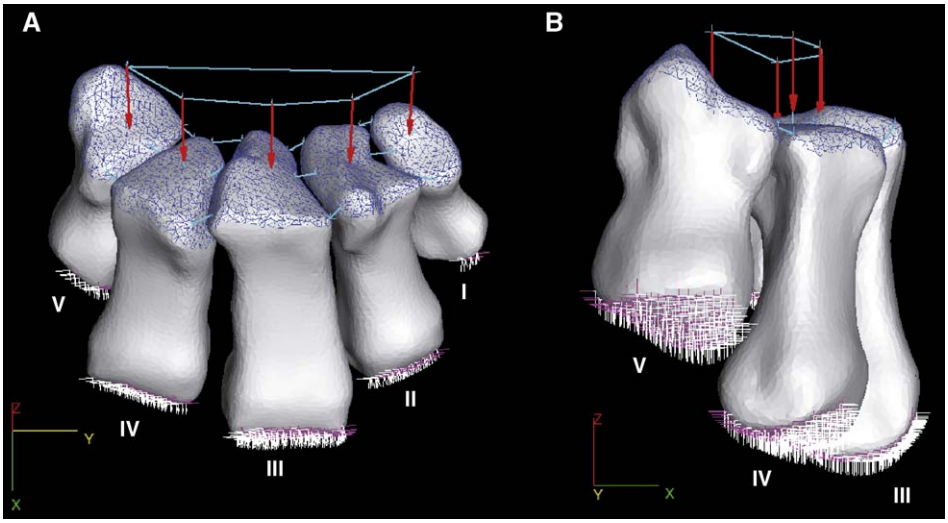

Fig. 1. Finite element model of the metacarpals of *Elephas maximus* in natural arrangement, assembled from computed tomography (CT) data, in anterior view (A) and lateral view (B). Wrist joint was modelled as a solid, static carpal assemblage (blue links). Loading direction (proximal red arrows) and constraint conditions (distal white crosses) correspond to the static analysis of the weight-bearing phase.
Fig. 1. Modèle en éléments finis des métacarpes d'*Elephas maximus*, selon l'arrangement naturel obtenu à partir des données de tomographie assistée par ordinateur, en vue antérieure (A) et vue latérale (B). Le poignet est modélisé en tant qu'assemblage carpien solide, statique (liens bleus). La direction de la force appliquée (flèches rouges proximales) et les conditions de contrainte (croix blanches distales) correspondent à l'analyse statique de la phase de support du poids.

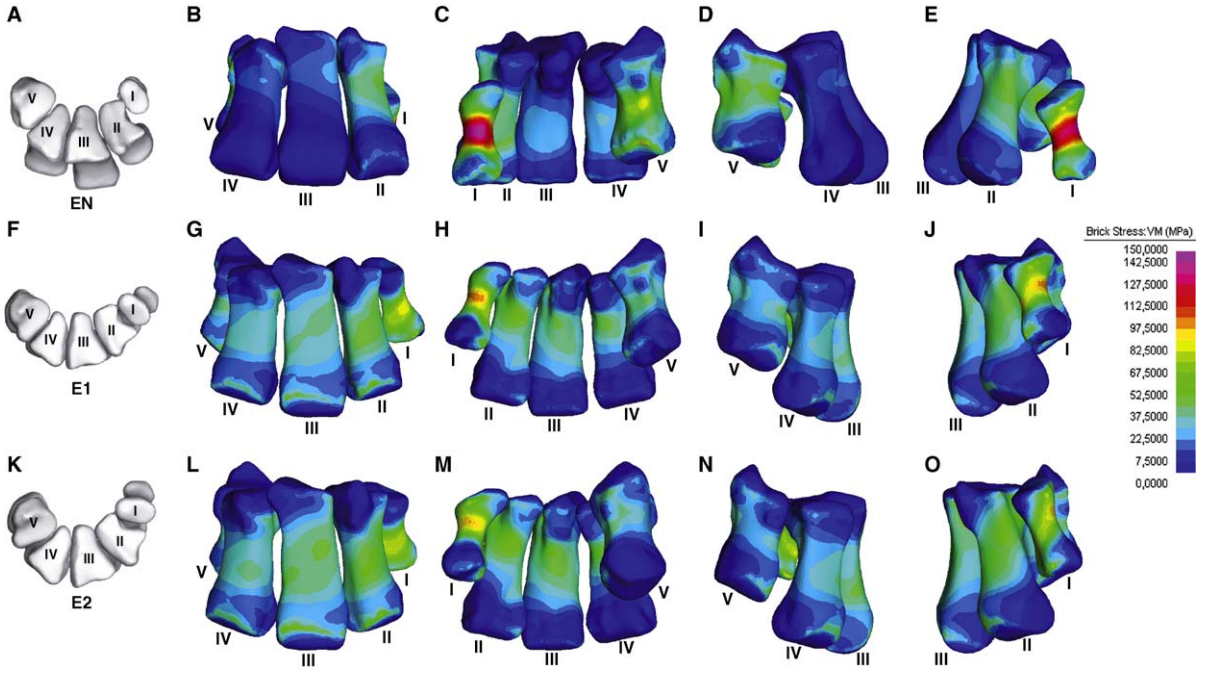

Fig. 2. The three metacarpal arrangements of *Elephas maximus* tested in this study, in proximal view: natural 'EN' (A) and fictitious 'E1' and 'E2' (F, K, respectively). von Mises stress distribution for natural arrangement EN (B–E), fictitious 'opened' arrangement E1 (G–J), and fictitious 'tubular' arrangement E2 (L–O), in anterior (B, G, L), posterior (C, H, M), lateral (D, I, N) and medial (E, J, O). Roman numbers indicate metacarpals.
Fig. 2. Les trois arrangements métacarpiens d'*Elephas maximus* testés dans ce travail, en vue proximale: arrangement naturel « EN » (A) et arrangements fictifs « E1 » et « E2 » (F, K, respectivement). Distribution du stress de von Mises pour l'arrangement naturel EN (B–E), pour l'arrangement fictif « ouvert » E1 (G–J), et pour l'arrangement fictif « tubulaire » E2 (L–O), en vues antérieure (B, G, L), postérieure (C, H, M), latérale (D, I, N) et médiale (E, J, O). Les chiffres romains indiquent les métacarpiens.

Table 1
Descriptive statistics (boxplot) from von Mises stress values (MPa). Mc: metacarpal; Min.: lower stress value; Med.: median stress value; Max.: highest stress value; Q1 and Q3, first and third quartile, respectively. Only stress values from metacarpal diaphyses' 'bricks' are taken, in order to avoid methodological artefacts (see text for details).
Tableau 1
Statistiques descriptives (*boxplot*) à partir des valeurs de stress de von Mises (en Mpa). Mc: métacarpien; Min.: valeur de stress minimale; Med.: valeur de stress médiane; Max.: valeur de stress maximale; Q1 and Q3, respectivement premier et troisième quartiles. Seules les valeurs de stress correspondant aux éléments de la diaphyse des métacarpiens sont considérées, afin d'éviter les artefacts méthodologiques (voir texte pour détails).

Metacarpal arrangement	Mc	Min.	Q1	Med.	Q3	Max.
EN	Total	0.2904	13.8800	19.9700	35.0000	156.7000
	McI	3.7860	33.3300	41.1600	46.4600	97.3200
	McII	0.2904	9.7190	14.3900	17.9400	33.1900
	McIII	0.5427	10.8900	14.6800	18.0100	31.2600
	McIV	4.6000	23.2700	29.6800	36.3200	55.8800
	McV	17.2300	76.0000	88.2400	99.1400	156.700
E1	Total	0.5546	23.6000	28.2700	33.7000	111.9000
	McI	6.5610	23.6900	26.3700	28.8000	51.8700
	McII	4.0900	21.7000	25.8500	29.8500	61.1900
	McIII	3.5490	24.4300	29.6500	33.9200	50.870
	McIV	0.5546	24.6400	31.8700	37.9300	64.9100
	McV	3.1940	46.2400	60.8300	69.8400	111.900
E2	Total	0.4865	23.1300	29.3300	36.9600	107.6000
	McI	0.6252	19.6800	23.5100	26.7600	50.2000
	McII	1.6770	22.3800	27.1700	30.9800	63.8000
	McIII	3.1600	27.8100	34.2800	38.9600	59.7100
	McIV	0.4865	24.8200	33.8000	40.4600	68.4400
	McV	3.4680	38.7500	55.6200	66.0100	107.600

  - a natural arrangement (EN, Fig. 2A), obtained directly from the CT data of the fresh limb,
  - an "open" arrangement (E1, Fig. 2F), by repositioning proximal surface of metacarpals on the same plane (particularly metacarpal I), with a more vertical orientation for the metacarpals II-IVm,
  - a slightly more "tubular" arrangement (E2, Fig. 2K), by increasing the angulation between metacarpals in proximal view from the open arrangement (E1). These metacarpal arrangements are inspired by the suspected arrangements for sauropod metacarpals;
- in absence of data from elephant bone, material properties are taken from published values (Reilly and Burstein, 1975) for fast-growing Haversian bovine bone (isotropic): density = 1.895 kg/m^3; elastic modulus (E) = 10 GPa; Poisson's ratio = 0.4; and shear modulus ($\mathbf{G}$) = 3.66 GPa. Because these models are homogeneous and linear (a single material property), other material properties will not be able to affect the stress distributions and magnitudes will remain proportional (Moreno et al., 2007);
- the load applied, 13,750 N per limb, is calculated from an estimation of 5.6 ton weight. This value represents a high estimation for adult elephants. We average an Asian elephant of 5 tons, with a specimen of exceptional size such as the naturalized elephant 'Siam' at the Muséum national d'histoire naturelle (6–7 tons). Despite the fact that the autopod used for the study was smaller (subadult specimen), we intended to push the limits of the structure, taking into account that the limbs do not only overcome body weight, but also dynamic loading during locomotion which amplifies the forces. Nevertheless, our model is linear static, and so it is a function between load and material property, which will show similar stress distributions independent of magnitudes (Moreno et al., 2007). Larger loads will only make the areas of high stress more visible;
- loading is applied normal to the joint surface (Fig. 1A, B), under the assumption that the cartilage and synovial capsule would transmit most normalized forces (Moreno et al., 2007). Mobility is constrained by fixing the distal joint in all directions (Fig. 1A, B), in order to simulate limitations on movement when the foot is in contact with the ground. These loading and constraint conditions correspond to a static analysis of the stance phase in locomotion (weight-bearing phase);
- in order to contrast the different metacarpal arrangements, comparative statistics were performed using von Mises stress values obtained for each brick element from FEA. The values were exported from STRAUS7 software (v2.3, 2004) and statistical analyses were performed with R GUI software (v2.4.0, free licence) and a specific module of analysis programmed by one of the authors (K. Moreno). Only the values of 'bricks' from the metacarpal diaphyses are taken. This precaution allows us to avoid the artefacts introduced in the model at both the loaded and the constrained surfaces, which are the proximal and distal epiphyses, respectively. Descriptive statistics were used to provide statistical summaries (boxplots) of the stress distribution in models. Boxplot allows to depict groups of numerical data through their five-number summaries (Table 1): the smallest observation (sample minimum), lower quartile (Q1), median (Q2), upper quartile (Q3), and largest observation (sample maximum). The use of the median was used as a criterion for comparison because it is less sensitive to extreme values than the average. Two approaches are used in order to characterize metacarpal arrangements. First, a 'global' approach based on the total brick stress values for each arrangement and a comparison between

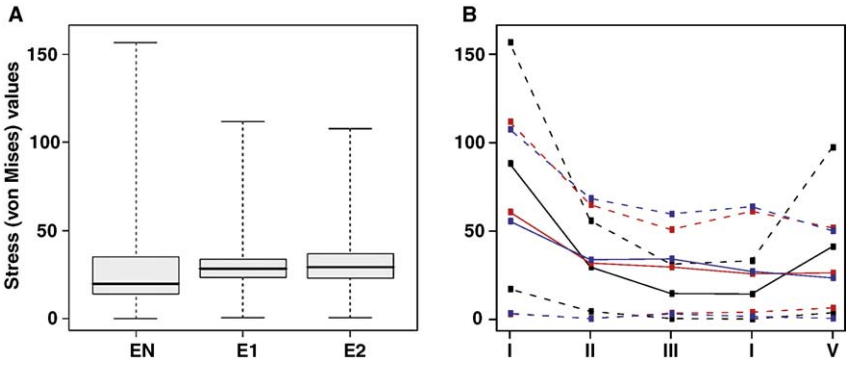

Fig. 3. Descriptive statistics from von Mises stress values for each metacarpal arrangement of *Elephas maximus*. (A) 'global' approach: boxplot based on the total brick stress values for each arrangement with 'EN', natural arrangement, 'E1' and 'E2', fictitious 'opened' and 'tubular' arrangements respectively, (B) 'individual' approach, stress profile based on boxplot values for each individual metacarpals with black line, natural arrangement 'EN', red line and blue line, fictitious arrangements 'E1' and 'E2', respectively. Continuous lines represent median stress values; superior and inferior dashed lines represent higher and lower stress values, respectively. Roman numbers indicate metacarpals.

Fig. 3. Statistiques descriptives à partir des valeurs de stress de von Mises pour chaque arrangement métacarpien d'*Elephas maximus*. (A) Approche « globale »: *boxplot* basé sur les valeurs de stress de l'ensemble des éléments pour chaque arrangement métacarpien avec « EN », l'arrangement naturel, « E1 » et « E2 », les arrangements fictifs « ouvert » et « tubulaire » respectivement, (B) approche « individuelle »: profil de stress basé sur les valeurs de *boxplot* pour chaque métacarpien individuel avec en noir, l'arrangement naturel « EN », en rouge et en bleu, les arrangements fictifs « E1 » et «E2 » respectivement. Les lignes continues représentent les valeurs de médiane de stress, les lignes pointillées supérieures et inférieures représentent les valeurs de stress maximales et minimales respectivement. Les chiffres romains indiquent les métacarpiens.

the three models. Second, an 'individual' approach based on the brick stress values for each individual metacarpal and a comparison between each arrangement. Because the compared value samples do not follow a normal distribution, but rather a one-tailed distribution, non-parametric Wilcoxon tests with paired samples are performed to compare each metacarpal arrangement with another one. These tests are computed in order to test if the stress value distributions differ significantly.

3. Results

The analyses of the three models reveal large differences between stress patterns of the natural metacarpal arrangement (Fig. 2B–E) and the modified ones (Fig. 2G–J and L–O). In natural configuration the highest stress is shown on McIV and V, whereas it seems more homogeneously distributed in all metacarpals of the two fictitious configurations. The comparative statistical analysis allows one to specify these differences:

- 'Global' approach (see above). The Wilcoxon tests revealed that observed differences between the three metacarpal arrangements were highly significant: E1 vs. E2 ($V = 5759770658$, $p\text{-value} < 2.2 \times 10^{-16}$), E1 vs. EN ($V = 11501993517$, $p\text{-value} < 2.2 \times 10^{-16}$) and E2 vs. EN ($V = 11610895239$, $p\text{-value} < 2.2 \times 10^{-16}$). This data suggests that the comparison between metacarpal arrangements shows a lower median (SGmed) stress in natural configuration than in both fictitious configurations (Fig. 3A Table 1). After modification of the metacarpal arrangement, we observe a significant increase of the SGmed, which increases toward the 'tubular' configuration (E2; +6% with regard to EN). Also, the SGmax tends to decrease with the 'opened' configuration (E1; −33% compared to EN), whereas the SGmin is not significatively affected. An important decrease of the interquartile range is also visible in fictitious arrangements;
- 'Individual' approach (see above). More precisely, the analysis of stress level in individual metacarpals permits to establish a "stress profile" for each model (Fig. 3B), which is another representation highlighting differences in stress pattern between arrangements. The study of the natural arrangement (EN) reveals a maximal concentration of stress in McI (higher SImed). In a general way, the stress concentrates on the medial (McI-II) and lateral (McV) parts of the hand. On the contrary, McII-III is slightly stressed with a lower SImed (only 13% of the median value of McI). Contrary to natural arrangement, both fictitious arrangements (E1, E2) present a general trend to decrease stress levels towards the lateral metacarpals, with McI always presenting the highest SImed. Also, the SImed variation for each metacarpals of the arrangements E1 and E2 present similar trends regarding the natural configuration, though with larger variation in the 'tubular' configuration (E2) SImed: decrease for McI and McV (in E2, respectively −37 and −43% compared to EN), and it increases for McII-IV (in E2, respectively +14, + 133 and 89% compared to EN).

4. Discussion

Our results confirm that the stress pattern cannot be solely referred to the morphology of the metacarpals, which remains unaltered, but it is a function of the metacarpal arrangement. A significant increase in the median level of stress is observed in the metacarpus when the natural arrangement is modified (E1, E2). Therefore the median appears as a potential good indicator of the most likely 'natural' metacarpal arrangement among the available possibilities. Similarly, the reduction of the

interquartile range around a higher median in the fictitious configurations E1 and E2 suggests an increase of zones at higher stress. On the other hand, an increasing interquartile range around a lower median in the natural metacarpal arrangement suggests that the bone is globally maintained at a lesser level of stress. However, the higher maximum intensity in this arrangement also suggests the presence of larger stressed zones, highly localized in the metacarpus.

Visualization of stress pattern and stress profile of the natural metacarpal arrangement allow us to specify the localization of these zones (Fig. 2B–E; Fig. 3B):

- the higher level of stress in McI and V, positioned posteriorly to McII-IV, suggests a redistribution of the stress in the posterior part of the metacarpus;
- these zones are clearly identified at mid-diaphysis and may correspond to regions presenting a higher risk of fracture. In real conditions, the presence of a well developed footpad might help overcome this problem redistributing the forces, probably by unloading the highly stressed posterior elements of the metacarpus (McI, McIV). However, FEA tests were not performed in this respect.

Interestingly, we can establish a parallel between these results and those of precedent studies about the structure of elephant autopods. Elephants have a cartilaginous medial element localized in the manus and pes footpad acting as a 'sixth digit' (Hutchinson et al., 2008; Weissengruber et al., 2006). Weissengruber et al. (2006) suggest this predigit assures a supportive function as a bone element modulating the footpad stiffness during the step, supplanting the "heel" in the subdigitigrad elephant manus. This stiffness modulation, allowed by the predigit action, could so play an important role in the unloading of the highly stressed posterior metacarpals (McI and McV) during the weight-bearing phase. The absence (no visualization on CT data) of the predigit in the specimen used in this study could be explained by an insufficient mineralization in a young specimen (Hutchinson et al., 2008). Despite the absence of an ossified predigit in the specimen used for modelling, our calculations indicate that, at loads encountered by a large adult, the palmar side of the metacarpals and particularly McI and McV get large stress. We could legitimately expect that the presence of the predigit would reduce the stress in the manus by redistributing the load on the metacarpals.

5. Conclusion

Our results indicate that it is possible to recognize the natural metacarpal arrangement of the extant Asian elephant among three different configurations by finding the stress distribution with the lowest median. Consequently, it is conceivable to use the same parameter to determine the most likely 'natural' metacarpal arrangement in extinct graviportal taxa where reconstitutions are debated such as sauropod dinosaurs.

High stress found in most posterior metacarpals of the Asian elephant can be linked with the presence of footpad and predigit. However, in absence of data on the exact influence of these elements (and other soft and connective tissues) on the stress distribution, our model can only reveal a rough stress pattern. However, this rough pattern is comparatively useful because in extinct taxa the soft tissues are usually not preserved. Nevertheless, our approach is potentially more informative in graviportal taxa whose footpad is absent, as in derived sauropods (Apesteguia, 2005; Christiansen, 1997; Wright, 2005). On the other hand, more tests are needed in order to use our method in non-graviportal taxa, since mechanical and structural characteristics (i.e., metacarpal orientation, limb posture) necessarily pose different loading/constraints conditions.

Acknowledgements

The authors thank John Hutchinson for his invaluable assistance in obtaining the CT scan data. This study was performed at the 3D platform of the Department "Histoire de la terre", UMR7207 CR2P CNRS "Centre de recherche sur la paléobiodiversité et les paléoenvironnements", Muséum National d'histoire naturelle. We thank Gaël Clément, Didier Geffard-Kuriyama and Philippe Taquet for the invitation to publish in this special volume. Helpful comments of three anonymous reviewers greatly improved the manuscript.

References

Anderson, D.D., Goldsworthy, J.K., Li, W., Rudert, J.M., Tochigi, Y., Brown, T.D., 2007. Physical validation of a patient-specific contact finite element model of the ankle. J. Biomech. 40 (8), 1662–1669.

Apesteguia, S., 2005. Evolution of the titanosaur metacarpus. In: Tidwell, V., Carpenter, K. (Eds.), Thunder-Lizards, The sauropodomorph dinosaurs. Indiana University Press, Bloomington, pp. 321–345.

Carrigan, S.D., Whiteside, R.A., Pichora, D.R., Small, C.F., 2003. Development of a three-dimensional finite element model for carpal load transmission in a static neutral posture. Ann. Biomed. Engin. 31 (6), 718–725.

Christian, A., Preuschoft, H., 1996. Deducing the body posture of extinct large vertebrates from the shape of the vertebral column. Palaeontology 39, 801–812.

Christiansen, P., 1997. Locomotion in sauropod dinosaurs. GAIA 14, 45–75.

Coombs, W.P., 1978. Theoretical aspects of cursorial adaptations in dinosaurs. Quart. Rev. Biol. 53 (4), 393–418.

Dar, F.H., Aspden, R.M., 2003. A finite element model of an idealized diarthrodial joint to investigate the effects of variation in the mechanical properties of the tissues. Proceedings of the Institution of Mechanical Engineers – Part H. J. Engin. Med. 217 (H5), 341–348.

Dumont, E.R., 2007. Feeding mechanisms in bats: variation within the constraints of flight. Integrat. Compar. Biol. 47, 137–146.

Dumont, E.R., Piccirillo, J., Grosse, I.R., 2005. Finite element analysis of biting behavior and bone stress in the facial skeletons of bats. Anatomical Record 293, 319–330.

Hutchinson, J.R., Miller, C.E., Fritsch, G., Hildebrandt, T., 2008. The anatomical foundation for multidisciplinary studies of animal limb function: examples from dinosaur and elephant limb imaging studies. In: Endo, H., Frey, R. (Eds.), Anatomical Imaging Techniques: towards a New Morphology. Springer-Verlag, Berlin, pp. 23–38.

Kupczik, K., Dobson, C.A., Crompton, R.H., Phillips, R., Oxnard, C.E., Fagan, M.J., O'Higgins, P., 2009. Masticatory loading and bone adaptation in the supraorbital torus of developing macaques. Am. J. Phys. Anthropol. 139 (2), 193–203.

Materialise MIMICS. v.13.1. 2009 Materialise. URL: http://www.materialise.com.

Moazen, M., Curtis, N., Evans, S.E., O'Higgins, P., Fagan, M.J., 2008. Combined finite element and multibody dynamics analysis of biting in a Uromastyx hardwickii lizard skull. J. Anat. 213, 499–508.

Moreno, K., Carrano, M.T., Snyder, R., 2007. Morphological changes in pedal phalanges through ornithopod dinosaur evolution: a biomechanical approach. J. Morphol. 268, 50–63.

Moreno, K., Wroe, S., Clausen, P., McHenry, C., d'Amore, D.C., Rayfield, E.J., Cunningham, E., 2008. Cranial performance in the Komodo dragon (*Varanus komodoensis*) as revealed by high-resolution 3-D finite element analysis. J. Anat. 212, 736–746.

Paul, G.S., Christiansen, P., 2000. 2000 Forelimb posture in neoceratopsian dinosaurs: implications for gait and locomotion. Paleobiology 26 (3), 450–465.

Rayfield, E., 2007. Finite element analysis and understanding the biomechanics and evolution of living and fossil organisms. Ann. Rev. Earth Planet. Sci. 35, 541–576.

Reggiani, B., Leardini, A., Corazza, F., Taylor, M., 2006. Finite element analysis of a total ankle replacement during the stance phase of gait. J. Biomech. 39 (8), 1435–1443.

Reilly, D.T., Burstein, A.H., 1975. Elastic and ultimate properties of compact bone tissue. J. Biomech. 8, 393–396.

Richmond, B.G., 2007. Biomechanics of phalangeal curvature. J. Human Evol. 53 (6), 678–690.

Richmond, B.G., Wright, B.W., Grosse, I., Dechow, P.C., Ross, C.F., Spencer, M.A., Strait, D.S., 2005. Finite element analysis in functional morphology. The Anatomical Record Part A: discoveries in Molecular, Cellular, and Evolutionary Biology 283A, 259–274.

STRAUS7. v.2.3. 2004 http://www.strand7.com/.

Tanner, J.B., Dumont, E.R., Sakai, S.T., Lundrigan, B.L., Holekamp, K.E., 2008. Of arcs and vaults: the biomechanics of bone-cracking in spotted hyenas (*Crocuta crocuta*). Biol. J. Linn. Soc. 95 (2), 246–255.

Weissengruber, G.E., Egger, G.F., Hutchinson, J.R., Groenewald, H.B., Elsässer, L., Famini, D., Forstenpointner, G., 2006. The structure of the cushions in the feet of African Elephants (Loxodonta africana). J. Anat. 209, 781–792.

Wright, J.L., 2005. Steps in Understanding Sauropod Biology: the importance of sauropod tracks. In: Curry Rogers, K.A., Wilson, J.A. (Eds.), The Sauropods: evolution and Paleobiology. University of California Press, Berkeley, pp. 252–284.

Wroe, S., 2008. High-resolution 3-D computer simulation of feeding behaviour in marsupial and placental lions. J. Zool. 274, 332–339.

Wroe, S., Huber, D.R., Lowry, M.B., McHenry, C.R., Moreno, K., Clausen, P.D., Ferrara, T.L., 2008. Three-dimensional computer analysis of white shark jaw mechanics: how hard can a great white bite? J. Zool. 276 (4), 336–342.

Wu, L., 2007. Nonlinear finite element analysis for musculoskeletal biomechanics of medial and lateral plantar longitudinal arch of Virtual Chinese Human after plantar ligamentous structure failures. Clinical Biomech. 22 (2), 221–229.